Optimized steering: Quantum state engineering and exceptional points

Parveen Kumar, Kyrylo Snizhko, Yuval Gefen, and Bernd Rosenow

Phys. Rev. A **105**, L010203 — Published 18 January 2022

DOI: 10.1103/PhysRevA.105.L010203

Optimized Steering: Quantum State Engineering and Exceptional Points

Parveen Kumar,[1] Kyrylo Snizhko,[2, 1] Yuval Gefen,[1] and Bernd Rosenow[3]

[1]*Department of Condensed Matter Physics, Weizmann Institute of Science, Rehovot 7610001, Israel*
[2]*Institute for Quantum Materials and Technologies, Karlsruhe Institute of Technology, 76021 Karlsruhe, Germany*
[3]*Institut für Theoretische Physik, Universität Leipzig, Brüderstrasse 16, 04103 Leipzig, Germany*

The state of a quantum system may be steered towards a predesignated target state, employing a sequence of weak *blind* measurements (where the detector's readouts are traced out). Here we analyze the steering of a two-level system using the interplay of a system Hamiltonian and weak measurements, and show that *any* pure or mixed state can be targeted. We show that the optimization of such a steering protocol is underlain by the presence of Liouvillian exceptional points. More specifically, for high purity target states, optimal steering implies purely relaxational dynamics marked by a second-order exceptional point, while for low purity target states, it implies an oscillatory approach to the target state. The dynamical phase transition between these two regimes is characterized by a third-order exceptional point.

Steering of a quantum system towards a pre-designated target state can be achieved either by drive-and-dissipation schemes [1–14] or through measurement-based protocols [15–21]. The former employ a dissipative environment to relax the quantum system into the target state, while in the latter case relaxation (as well as back-action on the system) is achieved by measurements. Optimizing the rate of convergence towards the target state is important to render it of practical importance and minimize external perturbations. Refs [22, 23] comprise a mathematical analysis of the steady states and the convergence speed. Exceptional points (EPs), referring to non-Hermitian degeneracies where two or more eigenvectors of the evolution operator coalesce [24–28], play an important role in a variety of optimization problems [29–35]. Such degeneracies are of particular interest in dynamics with complex eigenvalues where unitary dynamics competes with dissipation or gain, and may be generalized from non-Hermitian Hamiltonians to Liouvillian dynamics [36, 37]. In recent years, it has been recognized that operating near an EP enables unique functionality such as unidirectional invisibility [38–41] or enhanced sensitivity [42–47].

Here, we propose a family of protocols for steering a two-level quantum system towards desired target states. The system's initial state is assumed unknown to us. In our protocol, the quantum system is subject to both a Hamiltonian evolution and a measurement-induced evolution, and the combined effect of both can be described by a Liouvillian superoperator. The system's target state is given by the Liouvillian eigenstate having zero eigenvalue, and is uniquely determined (along with its purity) by the interplay between the Hamiltonian and the measurement protocol. When optimizing our steering [48] protocol in the sense that the target state is reached as fast as possible, we find that the optimal steering for high purity target states is dominated by the measurement-induced dynamics and described by second-order exceptional points, while optimal protocols for low purity target states are dominated by the system-Hamiltonian-induced dynamics. The transition between these two regimes is characterized by a third-order EP, where all three nonzero eigenvalues of the Liouvillian superoperator coalesce, and the optimal convergence dynamics of the system changes from non-oscillatory to oscillatory, reminiscent of a spontaneous breaking of $\mathcal{PT}$-symmetry [26, 49–53]. We note that, with a small cost in the target state purity, the steering rate can be significantly enhanced. In addition, we present an argument that the appearance of a higher-order exceptional point in the context of optimization is generic and applies to many-body systems as well.

On a more technical level, representing the system state on or within the Bloch sphere by a vector $\mathbf{s}$, its purity is characterized by $P \equiv (1+\mathbf{s}^2)/2$. We find that the optimal steering dynamics can be characterized by three different regimes, summarized in Fig. 2. In the low purity regime with $P \leq 7/8$, the convergence rate becomes optimal by choosing the Zeeman field in the system Hamiltonian as large as possible, and convergence towards the target state is oscillatory. In the medium purity regime, $7/8 < P \leq 127/128$, optimum convergence is achieved when all three non-vanishing eigenvalues of the Liouvillian superoperator have equal real parts; the optimal convergence rate is independent of P, while the convergence dynamics remains oscillatory, similar to the low purity regime. The transition to the high purity regime with $127/128 < P \leq 1$ occurs at a third-order EP where all three nonzero eigenvalues of the Liouvillian superoperator coalesce. In the high purity regime, the optimal convergence dynamics is non-oscillatory since all three nonzero eigenvalues of the superoperator are real, and two of them are degenerate, placing the superoperator at a conventional second-order EP.

System evolution and the steady state.— Consider a two-level quantum system represented by the density matrix ρ_s whose dynamics comprises two contributions: the unitary evolution and the measurement evolution. The former is governed by the following Hamiltonian acting in the system's Hilbert space

$$H_s = \omega\, \hat{n}\cdot\boldsymbol{\sigma}, \quad \hat{n} = (\cos\phi\sin\theta, \sin\phi\sin\theta, \cos\theta), \quad (1)$$

where ω is the Zeeman energy of the two levels, θ, ϕ are spherical coordinates parametrizing the unit vector $\hat{n}$, and $\boldsymbol{\sigma} = (\sigma_x, \sigma_y, \sigma_z)$ is the vector of Pauli matrices.

For the measurement evolution, the system needs to couple with the detector, which is chosen to be a two-level quantum object prepared in the state $\rho_d^0 = \frac{1}{2}(\mathbb{I} + \hat{m}\cdot\boldsymbol{\sigma})$, where $\hat{m}$ is the detector state initialization direction. Before they interact, the joint system-detector state is $\rho(t) = \rho_s(t)\otimes\rho_d^0$. At later times, the joint state $\rho(t)$ evolves with the system-detector interaction Hamiltonian

$$H_{s-d} = J\left[\boldsymbol{\sigma}^s\cdot\boldsymbol{\sigma}^d - (\hat{m}\cdot\boldsymbol{\sigma}^s)(\hat{m}\cdot\boldsymbol{\sigma}^d)\right], \quad (2)$$

where J is the coupling parameter, and $\boldsymbol{\sigma}^s$, $\boldsymbol{\sigma}^d$ are the pseudo-spin operators of the system and detector, respectively. Then the interaction is switched off, and the detector state is measured projectively; disentangling the composite system-detector state and generating a measurement back-action on the system state $\rho_s(t)$. In our *blind measurement* protocol [20], the detector readouts are discarded (i.e., traced out). After each measurement step, the detector state is reset to ρ_d^0. We note that the system-detector interaction is chosen to be anisotropic, such that only the system's spin direction orthogonal to the detector state initialization direction is coupled.

In our dynamics, the Hamiltonian evolution (cf. Eq. (1)) and the measurement evolution (cf. Eq. (2)) happen simultaneously. Over a small time step dt, the two processes do not interfere with each other (up to $O(dt)$). An infinitesimal time step evolution of the system is given by $\rho_s(t+dt) = \mathrm{tr_d}[e^{-iHdt}\rho(t)e^{iHdt}]$ where $H = H_s\otimes\mathbb{I} + H_{s-d}$. In the continuous time limit $dt\to 0$, and using a scaling of J such that $J^2 dt = \text{const} \equiv \alpha$, we obtain [20, 21]

$$\frac{d\rho_s}{dt} = \mathcal{L}[\rho_s] = i\left[\rho_s, H_s\right] - 2\alpha\left(L^\dagger L\rho_s + \rho_s L^\dagger L - 2L\rho_s L^\dagger\right), \quad (3)$$

where $\mathcal{L}$ is the Liouvillian superoperator, α specifies the measurement strength, and $L = |\hat{m}_+\rangle\langle\hat{m}_-|$ is the Lindblad jump operator with $|\hat{m}_\pm\rangle$ as the eigenstates of the operator $\hat{m}\cdot\boldsymbol{\sigma}$ with eigenvalues ± 1.

The combined unitary and weak-measurement time evolution ultimately steer the system towards a steady state determined by the condition $d\rho_s^{(T)}/dt = \mathcal{L}[\rho_s^{(T)}] = 0$. We parameterize the steady state as $\rho_s^{(T)} = \frac{1}{2}(\mathbb{I} + \boldsymbol{s}\cdot\boldsymbol{\sigma})$ where $\boldsymbol{s} = (s_x, s_y, s_z)$ is the steady state Bloch vector. Assuming a detector state initialization $\hat{m} = (0,0,1)$, this steady state is given by

$$s_x = \frac{2\Omega\sin\theta(\Omega\cos\theta\cos\phi + \sin\phi)}{2 + \Omega^2(\cos^2\theta + 1)}, \quad (4a)$$

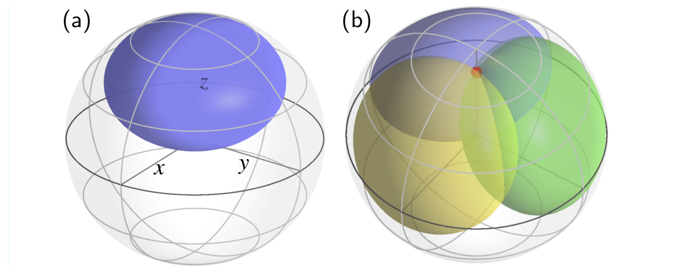

Figure 1. (a) Steady state ellipsoid for the detector state initialization direction $\hat{m} = (0,0,1)^T$, see Eq. (4). (b) The steady state ellipsoid can be rotated by rotating the detector state initialization direction. Hence, any target state (red) on or inside the Bloch sphere can be reached, as it lies on one or several rotated ellipsoids (e.g. blue, green, yellow).

$$s_y = \frac{2\Omega\sin\theta(\Omega\cos\theta\sin\phi - \cos\phi)}{2 + \Omega^2(\cos^2\theta + 1)}, \quad (4b)$$

$$s_z = \frac{2(1 + \Omega^2\cos^2\theta)}{2 + \Omega^2(\cos^2\theta + 1)}, \quad (4c)$$

where $\Omega = \omega/\alpha$. The steady state coordinates (cf. Eq. (4)) form an ellipsoid centered at the point $\hat{m}/2$, in this case $s_x^2 + s_y^2 + 2(s_z - 1/2)^2 = 1/2$; conversely, every state on this ellipsoid is obtained for at least one choice of the Zeeman field (Ω, θ, ϕ) [Fig. 1(a)]. The main features of the steady state ellipsoid are as follows: (i) it remains fully confined within the Bloch sphere, (ii) its shape remains independent of the protocol parameters, (iii) its minor axis starts from the center of the Bloch sphere and ends on its surface, coinciding with the detector state initialization direction $\hat{m}$, implying that there exists only one pure target state on a given ellipsoid. Each specific choice of protocol parameters (Ω, θ, ϕ) steers the system to a unique steady state on this ellipsoid, but the converse is not true as a given target state may be stabilized by several distinct sets (Ω, θ, ϕ). Furthermore, a given steady state may belong to several ellipsoids with different $\hat{m}$, and in that case, the minor axis (which is determined by $\hat{m}$) of each of these ellipsoids must have a fixed angle with regard to the Bloch vector $\boldsymbol{s}$ of the steady state (cf. Fig. 1(b)).

Rotating the detector state initialization direction $\hat{m}$, rotates the ellipsoid. Using all possible $\hat{m}$, the entire Bloch sphere (both surface and interior) can be covered by the ellipsoids, cf. Fig. 1(b). Therefore, any state, irrespective of its purity, can be targeted using our protocol.

Optimal steering.— Our aim now is to optimize the protocol such that the target state is reached as fast as possible. While the target state $\rho_s^{(T)}$ corresponds to the eigenvector with zero eigenvalue of the Liouvillian, $\mathcal{L}[\rho_s^{(T)}] = \lambda_0\rho_s^{(T)}$ with $\lambda_0 = 0$, the dynamical evolution of an arbitrary state is governed by the eigenvectors $\rho_s^{(j)}$ with nonzero eigenvalues λ_j, i.e. $\rho_s(t) =$

$\rho_s^{(T)} + \sum_j c_j \rho_s^{(j)} e^{\lambda_j t}$ where the coefficients c_j are determined by the system's initial state $\rho_s(0)$. Therefore, the deviations from the target state decay exponentially in time, and the decay rates are determined by the real parts of the nonzero eigenvalues of the superoperator $\mathcal{L}$. The smallest (in magnitude) nonzero real part, i.e. the inverse of the Liouvillian gap, determines the slowest convergence rate (Γ), and our aim is to maximize it by choosing appropriate parameters in the protocol. At first sight, a straightforward way to speed up the steering process would be to increase the measurement strength α, as the Liouvillian eigenvalues are directly proportional to it. However, $\alpha = J^2 dt$ is generically limited by the weak measurement constraint $(Jdt)^2 \ll 1$ and by the fact that the experimental measurement and readout time dt cannot be made arbitrarily short. Therefore, we consider α to be fixed at some maximum strength. The protocol parameters that can still be optimized are the initialization direction $\hat{m}$ and the system Hamiltonian specified by Ω, θ and ϕ. These, however, are partially constrained by the choice of a specific target state. The optimization problem simplifies further by noting that the Liouvillian eigenvalues remain invariant under a unitary rotation of the system state [54]. Thus, without loss of generality, we analyze the problem by selecting $\hat{m} = (0, 0, 1)$, for which the steady state is given by Eq. (4) with the corresponding steady state ellipsoid shown in Fig. 1(a). Since different states having the same purity are related via a unitary transformation, all target states on a given ellipsoid having the same purity possess the same convergence rate. This leaves us with two significant parameters: θ and Ω. We treat Ω as an independent parameter, while θ is determined by Ω and the target state purity P. Note that, using the ellipsoid equation, the purity of a steady state can be expressed as $P = 1 - (1 - s_z)^2/2$. For each target state purity P, we aim to tune the free parameter Ω such that the convergence rate Γ becomes optimal. However, we note that, for a given target state, there exists a lower bound on the allowed values of Ω, which is an important constraint on the optimization problem [54].

The optimal convergence rate and its dependence on the target state purity are obtained numerically, and are shown in Fig. 2(a). We solve the eigenvalue equation $\mathcal{L}[\rho_s] = \lambda\, \rho_s$ and focus on the eigenvalue having smallest (in magnitude) real part which we maximize over all admissible values of Ω. We find that the conditions for optimal convergence depend on the degree of purity of the target state — we identify a low, medium and high purity regime, Fig. 2(a). In the low purity regime, the convergence rate becomes bigger the further Ω is increased, implying that steering becomes optimal by choosing Ω as large as possible, Fig. 2(b). In the medium purity regime, we find a critical Ω at which all three nonzero eigenvalues of $\mathcal{L}$ have equal real part, and the convergence rate becomes optimal at this critical Ω, Fig. 2(c). The transition from the medium to the high purity regime is marked by the fact that at this critical Ω, not only the real parts, but also the imaginary parts of the three nonzero eigenvalues of $\mathcal{L}$ coincide — the convergence rate becomes optimal at a third-order EP where all three nonzero eigenvalues of $\mathcal{L}$ coincide, Fig. 2(d). In the high purity regime, we find optimal convergence for a critical Ω where $\mathcal{L}$ encounters a second-order EP, Fig. 2(e). Intuitively, one can understand the optimized convergence rate behavior in the following way. The protocol targeting any mixed state (with purity P less than 1) involves an interplay of the relaxation to a pure state (controlled by α) and Hamiltonian rotation (controlled by ω). Relaxation happening probabilistically at different moments in time, combined with the Hamiltonian rotation of the newly-relaxed states, leads to the desired mixed state. For target states with sufficiently large purities, there is an optimal ratio $\Omega = \omega/\alpha$, when the convergence is the fastest. Whereas for sufficiently small purities, the approach to the target state is limited by the speed of "mixing", so that it is the faster, the larger Ω is. The optimal approach to the target state is oscillatory in the low and medium purity regimes, as two of the eigenvalues have nonzero imaginary parts for all values of Ω, Fig. 2(b,c). By contrast, the optimal approach to the target state becomes non-oscillatory (exponential decay) in the high purity regime, because all three eigenvalues of the Liouvillian are real at the optimal value of Ω, Fig. 2(e). Analytical results for the transitions between regimes and the optimal convergence rates are presented in the supplemental material [54].

We highlight that the central feature of our system is a dynamical phase transition at the target state purity $P = 127/128$ from Hamiltonian-dominated, oscillatory to measurement-dominated, non-oscillatory dynamics. This transition proceeds through a *third-order* EP where all three nonzero eigenvalues of the Liouvillian superoperator coincide; the eigenvalues are obtained as [54]: $\lambda_1 = \lambda_2 = \lambda_3 = -8\alpha/3$. While dynamical phase transitions have been associated with second-order EPs, for instance in $\mathcal{PT}$-symmetric systems [26, 51, 55], the natural appearance of a third-order EP seems striking.

To understand why optimal steering is related to a third-order EP, we now present a general principle for optimization. To explain this principle, we first shift our perspective and ask: Comparing the target states in different regimes, what is the fastest possible convergence rate that can be achieved? It can be shown that, in general, the *average* of the decay rates (i.e., the trace of the Liouvillian superoperator) depends only on the dissipative channels and not on the system Hamiltonian [56]. In our protocol we fix the average to be $8\alpha/3$. Evidently, if one decay rate is above average, then another one is necessarily below average; therefore, the optimum convergence rate is achieved when all decay rates are equal (to this average) which naturally happens at the EPs. In our protocol this is realized in the medium purity regime

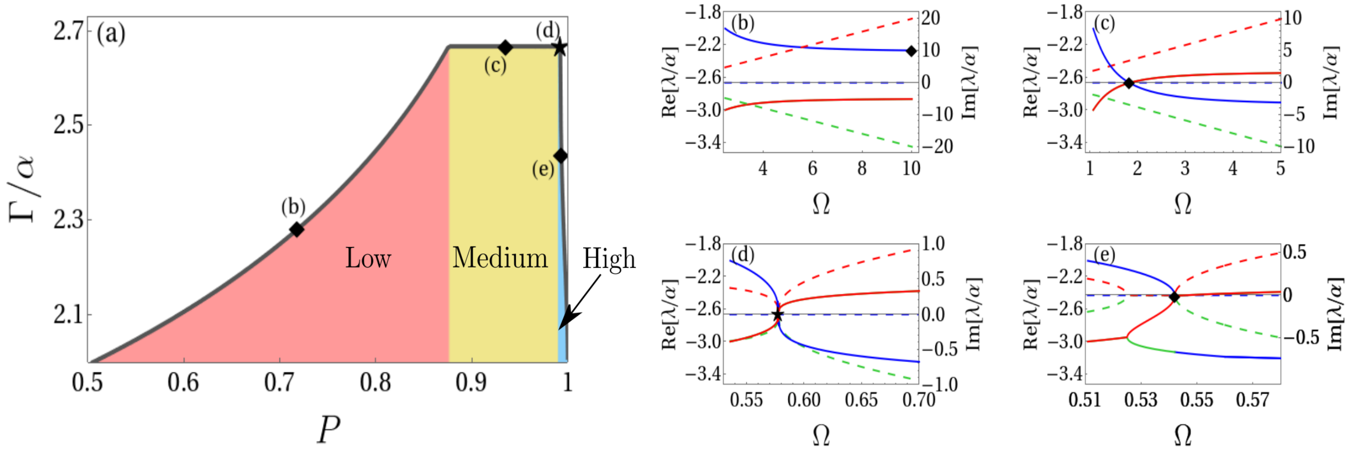

Figure 2. Optimal convergence rate Γ in units of the measurement strength α as a function of target state purity P (a). We identify three regimes: A low purity regime $1/2 \leq P \leq 7/8$, a medium purity regime $7/8 < P \leq 127/128$, and a high purity regime $127/128 < P \leq 1$. Choosing one target state from each different purity regime (marked by ♦ in (a)), we plot the real (solid) and imaginary (dashed) parts of the nonzero eigenvalues λ of the Liouvillian superoperator as a function of Ω in (b), (c) and (e). Here, $\Omega = \omega/\alpha$ is the ratio of the Zeeman energy ω of the system Hamiltonian, Eq. (1), to the measurement strength α, Eq. (3). Note that the eigenvalues λ may be real or come in complex-conjugate pairs; in the latter case, the red and the green lines, showing Re λ of the two complex-conjugate eigenvalues, coincide. Panel (e) contains a segment where all three eigenvalues are real; there all three colors appear explicitly in the plot. Steering becomes optimal when the parameter Ω is tuned such that the topmost real part (solid) becomes as negative as possible (marked by ♦). At the transition from the medium to the high purity (marked by $\star$ in (a)), the optimal convergence rate occurs at a third-order EP shown in (d).

(cf. Fig 2(a)). In fact, in this regime the convergence rate plateaus at an upper limit that is given by the *average* of the decay rates. In the other regimes, there is no value of Ω for which all three decay rates become equal simultaneously. We thus conclude that steering is necessarily optimal at the third-order EP, because the equality of all three nonzero eigenvalues entails the equality of the decay rates.

One expects the above considerations to be applicable to broad classes of systems, including dissipative many-body platforms [56]. The presence of additional (unwanted) dissipative channels beyond those required by the protocol can modify the optimal steering rate. However, we still expect the optimality to be associated with an exceptional point.

Experimental implementation.—Our protocol can be implemented in a variety of experimental platforms. The main ingredient of our protocol, blind measurements stabilizing the system at a specific pure state, is particularly natural for implementation in cold atomic systems such as cold ions [57] or Rydberg atoms [58], but is also supported by fluxonium [59–61] and transmon qubits [35]. High-fidelity coherent Hamiltonian manipulation in these systems is now routinely performed in many laboratories [62–64]. Combining the ingredients and implementing our protocol in these systems appears straightforward. Checking our predictions for the steering optimality and its relation to EPs, however, will require a degree of control and stability in the system beyond the standard levels, as the system sensitivity to perturbations in the vicinity of EPs is expected to be enhanced [42, 44, 45, 65].

Conclusion.— We have proposed a steering protocol which uses the interplay of a unitary and a weak-measurement-induced evolution to steer a two-level quantum system towards any desired target state on or within the Bloch sphere. The resulting Lindbladian dominates the steering towards high purity states, while the Hamiltonian dynamics dominates the optimal steering towards low purity mixed states. In all cases the optimum convergence rate is linked with exceptional points of the Liouvillian. The latter exhibits a dynamical phase transition such that the dynamics changes from oscillatory to exponential decaying. This transition is characterized by the presence of a third-order EP.

The convergence rate optimization analysis in our work suggests that a significant speedup can be achieved with a slight compromise in the target state purity. This implies that it may be beneficial to target a state that is not exactly the desired one (e.g., has 99% purity), so that convergence can be sped up significantly. Faster convergence will leave less time for unavoidable noise to affect the system dynamics, thus improving the target state fidelity. This may prove significant for recent state stabilization protocols [8–10, 14].

Note added.— In a recent work [66], Khandelwal et al. have discussed the relevance of EPs for optimal operation of quantum thermal machines.

We would like to thank Heinrich-Gregor Zirnstein for collaboration on an earlier version of this manuscript. This project was supported by the Deutsche Forschungsgemeinschaft (DFG, German Research Foundation) — 277101999 — TRR 183 (project C01), EG 96/13-1 and GO 1405/6-1, by the Israel Science Foundation (ISF), and by the National Science Foundation through award DMR-2037654 and the US–Israel Binational Science Foundation (BSF), Jerusalem, Israel. Y.G. acknowledges support by the Helmholtz International Fellow Award.

[1] S. Diehl, A. Micheli, A. Kantian, B. Kraus, H. P. Büchler, and P. Zoller, Quantum states and phases in driven open quantum systems with cold atoms, Nature Physics **4**, 878 (2008).

[2] B. Kraus, H. P. Büchler, S. Diehl, A. Kantian, A. Micheli, and P. Zoller, Preparation of entangled states by quantum Markov processes, Physical Review A **78**, 042307 (2008).

[3] M. Roncaglia, M. Rizzi, and J. I. Cirac, Pfaffian State Generation by Strong Three-Body Dissipation, Physical Review Letters **104**, 096803 (2010).

[4] S. Diehl, E. Rico, M. A. Baranov, and P. Zoller, Topology by dissipation in atomic quantum wires, Nature Physics **7**, 971 (2011).

[5] A. Pechen, Engineering arbitrary pure and mixed quantum states, Physical Review A **84**, 042106 (2011).

[6] K. W. Murch, U. Vool, D. Zhou, S. J. Weber, S. M. Girvin, and I. Siddiqi, Cavity-Assisted Quantum Bath Engineering, Physical Review Letters **109**, 183602 (2012).

[7] Z. Leghtas, U. Vool, S. Shankar, M. Hatridge, S. M. Girvin, M. H. Devoret, and M. Mirrahimi, Stabilizing a Bell state of two superconducting qubits by dissipation engineering, Physical Review A **88**, 023849 (2013).

[8] S. Shankar, M. Hatridge, Z. Leghtas, K. M. Sliwa, A. Narla, U. Vool, S. M. Girvin, L. Frunzio, M. Mirrahimi, and M. H. Devoret, Autonomously stabilized entanglement between two superconducting quantum bits, Nature **504**, 419 (2013).

[9] Y. Lin, J. P. Gaebler, F. Reiter, T. R. Tan, R. Bowler, A. S. Sørensen, D. Leibfried, and D. J. Wineland, Dissipative production of a maximally entangled steady state of two quantum bits, Nature **504**, 415 (2013).

[10] Y. Liu, S. Shankar, N. Ofek, M. Hatridge, A. Narla, K. M. Sliwa, L. Frunzio, R. J. Schoelkopf, and M. H. Devoret, Comparing and Combining Measurement-Based and Driven-Dissipative Entanglement Stabilization, Physical Review X **6**, 011022 (2016).

[11] N. Goldman, J. C. Budich, and P. Zoller, Topological quantum matter with ultracold gases in optical lattices, Nature Physics **12**, 639 (2016).

[12] Y. Lu, S. Chakram, N. Leung, N. Earnest, R. K. Naik, Z. Huang, P. Groszkowski, E. Kapit, J. Koch, and D. I. Schuster, Universal Stabilization of a Parametrically Coupled Qubit, Physical Review Letters **119**, 150502 (2017).

[13] Z. Huang, Y. Lu, E. Kapit, D. I. Schuster, and J. Koch, Universal stabilization of single-qubit states using a tunable coupler, Physical Review A **97**, 062345 (2018).

[14] K. P. Horn, F. Reiter, Y. Lin, D. Leibfried, and C. P. Koch, Quantum optimal control of the dissipative production of a maximally entangled state, New Journal of Physics **20**, 123010 (2018).

[15] A. Pechen, N. Il'in, F. Shuang, and H. Rabitz, Quantum control by von Neumann measurements, Physical Review A **74**, 052102 (2006).

[16] L. Roa, A. Delgado, M. L. Ladrón de Guevara, and A. B. Klimov, Measurement-driven quantum evolution, Physical Review A **73**, 012322 (2006).

[17] L. Roa, M. L. L. de Guevara, A. Delgado, G. Olivares-Rentería, and A. B. Klimov, Quantum evolution by discrete measurements, Journal of Physics: Conference Series **84**, 012017 (2007).

[18] K. Jacobs, Feedback control using only quantum back-action, New Journal of Physics **12**, 043005 (2010).

[19] S. Ashhab and F. Nori, Control-free control: Manipulating a quantum system using only a limited set of measurements, Physical Review A **82**, 062103 (2010).

[20] S. Roy, J. T. Chalker, I. V. Gornyi, and Y. Gefen, Measurement-induced steering of quantum systems, Physical Review Research **2**, 033347 (2020).

[21] P. Kumar, K. Snizhko, and Y. Gefen, Engineering two-qubit mixed states with weak measurements, Physical Review Research **2**, 042014 (2020).

[22] F. Ticozzi, R. Lucchese, P. Cappellaro, and L. Viola, Hamiltonian Control of Quantum Dynamical Semigroups: Stabilization and Convergence Speed, IEEE Transactions on Automatic Control **57**, 1931 (2012).

[23] B. Baumgartner and H. Narnhofer, Analysis of quantum semigroups with GKS–Lindblad generators: II. General, Journal of Physics A: Mathematical and Theoretical **41**, 395303 (2008).

[24] T. Kato, *Perturbation Theory for Linear Operators*, Classics in Mathematics, Vol. 132 (Springer Berlin Heidelberg, Berlin, Heidelberg, 1995).

[25] M. Berry, Physics of Nonhermitian Degeneracies, Czechoslovak Journal of Physics **54**, 1039 (2004).

[26] W. D. Heiss, The physics of exceptional points, Journal of Physics A: Mathematical and Theoretical **45**, 444016 (2012).

[27] N. Hatano, Exceptional points of the Lindblad operator of a two-level system, Molecular Physics **117**, 2121 (2019).

[28] F. Minganti, A. Miranowicz, R. W. Chhajlany, and F. Nori, Quantum exceptional points of non-Hermitian Hamiltonians and Liouvillians: The effects of quantum jumps, Physical Review A **100**, 062131 (2019).

[29] Z. Lin, A. Pick, M. Lončar, and A. W. Rodriguez, Enhanced Spontaneous Emission at Third-Order Dirac Exceptional Points in Inverse-Designed Photonic Crystals, Physical Review Letters **117**, 107402 (2016).

[30] A. Lupu, V. V. Konotop, and H. Benisty, Optimal PT-symmetric switch features exceptional point, Scientific Reports **7**, 13299 (2017).

[31] A. Metelmann and H. E. Türeci, Nonreciprocal signal routing in an active quantum network, Physical Review A **97**, 043833 (2018).

[32] M. Partanen, J. Goetz, K. Y. Tan, K. Kohvakka, V. Sevriuk, R. E. Lake, R. Kokkoniemi, J. Ikonen, D. Hazra, A. Mäkinen, E. Hyyppä, L. Grönberg, V. Vesterinen, M. Silveri, and M. Möttönen, Exceptional points in tunable superconducting resonators, Physical Review B **100**, 134505 (2019).

[33] L. J. Fernández-Alcázar, R. Kononchuk, and T. Kottos,

Thermal Motors with Enhanced Performance due to Engineered Exceptional Points, (2020), arXiv:2010.06743.

[34] J. Wiersig, Robustness of exceptional-point-based sensors against parametric noise: The role of Hamiltonian and Liouvillian degeneracies, Physical Review A **101**, 053846 (2020).

[35] W. Chen, M. Abbasi, Y. N. Joglekar, and K. W. Murch, Quantum jumps in the non-Hermitian dynamics of a superconducting qubit, **2**, 1 (2021), arXiv:2103.06274.

[36] F. Minganti, A. Miranowicz, R. W. Chhajlany, I. I. Arkhipov, and F. Nori, Hybrid-Liouvillian formalism connecting exceptional points of non-Hermitian Hamiltonians and Liouvillians via postselection of quantum trajectories, Physical Review A **101**, 062112 (2020).

[37] I. I. Arkhipov, A. Miranowicz, F. Minganti, and F. Nori, Liouvillian exceptional points of any order in dissipative linear bosonic systems: Coherence functions and switching between $\mathcal{PT}$ and anti- $\mathcal{PT}$ symmetries, Physical Review A **102**, 033715 (2020).

[38] Z. Lin, H. Ramezani, T. Eichelkraut, T. Kottos, H. Cao, and D. N. Christodoulides, Unidirectional Invisibility Induced by PT -Symmetric Periodic Structures, Physical Review Letters **106**, 213901 (2011).

[39] A. Regensburger, C. Bersch, M.-A. Miri, G. Onishchukov, D. N. Christodoulides, and U. Peschel, Parity–time synthetic photonic lattices, Nature **488**, 167 (2012).

[40] L. Feng, Y.-L. Xu, W. S. Fegadolli, M.-H. Lu, J. E. B. Oliveira, V. R. Almeida, Y.-F. Chen, and A. Scherer, Experimental demonstration of a unidirectional reflectionless parity-time metamaterial at optical frequencies, Nature Materials **12**, 108 (2013).

[41] B. Peng, a. K. Özdemir, F. Lei, F. Monifi, M. Gianfreda, G. L. Long, S. Fan, F. Nori, C. M. Bender, and L. Yang, Parity–time-symmetric whispering-gallery microcavities, Nature Physics **10**, 394 (2014).

[42] J. Wiersig, Enhancing the Sensitivity of Frequency and Energy Splitting Detection by Using Exceptional Points: Application to Microcavity Sensors for Single-Particle Detection, Physical Review Letters **112**, 203901 (2014).

[43] Z.-P. Liu, J. Zhang, a. K. Özdemir, B. Peng, H. Jing, X.-Y. Lü, C.-W. Li, L. Yang, F. Nori, and Y.-x. Liu, Metrology with PT-Symmetric Cavities: Enhanced Sensitivity near the PT-Phase Transition, Physical Review Letters **117**, 110802 (2016).

[44] H. Hodaei, A. U. Hassan, S. Wittek, H. Garcia-Gracia, R. El-Ganainy, D. N. Christodoulides, and M. Khajavikhan, Enhanced sensitivity at higher-order exceptional points, Nature **548**, 187 (2017).

[45] W. Chen, a. Kaya Özdemir, G. Zhao, J. Wiersig, and L. Yang, Exceptional points enhance sensing in an optical microcavity, Nature **548**, 192 (2017).

[46] H.-K. Lau and A. A. Clerk, Fundamental limits and non-reciprocal approaches in non-Hermitian quantum sensing, Nature Communications **9**, 4320 (2018).

[47] M. Zhang, W. Sweeney, C. W. Hsu, L. Yang, A. D. Stone, and L. Jiang, Quantum Noise Theory of Exceptional Point Amplifying Sensors, Physical Review Letters **123**, 180501 (2019).

[48] In this paper, we use the word “steering” as the name of a process that leads an arbitrary initial state of the system to a predesignated target state. This should not be confused with “steering” from the theory of quantum information and quantum computation which defines a special kind of nonlocal correlations.

[49] C. M. Bender and S. Boettcher, Real Spectra in Non-Hermitian Hamiltonians Having PT Symmetry, Physical Review Letters **80**, 5243 (1998).

[50] C. M. Bender, Making sense of non-Hermitian Hamiltonians, Reports on Progress in Physics **70**, 947 (2007).

[51] R. El-Ganainy, K. G. Makris, M. Khajavikhan, Z. H. Musslimani, S. Rotter, and D. N. Christodoulides, Non-Hermitian physics and PT symmetry, Nature Physics **14**, 11 (2018).

[52] C. M. Bender, P. E. Dorey, C. Dunning, A. Fring, D. W. Hook, H. F. Jones, S. Kuzhel, G. Lévai, and R. Tateo, *PT Symmetry: In Quantum and Classical Physics* (World Scientific (Europe), 2019) Chap. 1.

[53] Y. Ashida, Z. Gong, and M. Ueda, Non-Hermitian Physics, arXiv (2020), arXiv:2006.01837.

[54] See the Supplemental Material where we derive the lower bound on allowed Ω and obtain the optimal convergence rate.

[55] Ş. K. Özdemir, S. Rotter, F. Nori, and L. Yang, Parity-time symmetry and exceptional points in photonics, Nat. Mater. **18**, 783 (2019).

[56] H.-G. Zirnstein, unpublished.

[57] E. Ben Av, Y. Shapira, N. Akerman, and R. Ozeri, Direct reconstruction of the quantum-master-equation dynamics of a trapped-ion qubit, Physical Review A **101**, 062305 (2020).

[58] H. Weimer, M. Müller, I. Lesanovsky, P. Zoller, and H. P. Büchler, A Rydberg quantum simulator, Nature Physics **6**, 382 (2010).

[59] I. M. Pop, K. Geerlings, G. Catelani, R. J. Schoelkopf, L. I. Glazman, and M. H. Devoret, Coherent suppression of electromagnetic dissipation due to superconducting quasiparticles, Nature **508**, 369 (2014).

[60] N. Earnest, S. Chakram, Y. Lu, N. Irons, R. K. Naik, N. Leung, L. Ocola, D. A. Czaplewski, B. Baker, J. Lawrence, J. Koch, and D. I. Schuster, Realization of a Λ System with Metastable States of a Capacitively Shunted Fluxonium, Phys. Rev. Lett. **120**, 150504 (2018).

[61] T. M. Hazard, A. Gyenis, A. Di Paolo, A. T. Asfaw, S. A. Lyon, A. Blais, and A. A. Houck, Nanowire Superinductance Fluxonium Qubit, Phys. Rev. Lett. **122**, 010504 (2019).

[62] M. Saffman, T. G. Walker, and K. Mølmer, Quantum information with Rydberg atoms, Reviews of Modern Physics **82**, 2313 (2010).

[63] I. S. Madjarov, J. P. Covey, A. L. Shaw, J. Choi, A. Kale, A. Cooper, H. Pichler, V. Schkolnik, J. R. Williams, and M. Endres, High-fidelity entanglement and detection of alkaline-earth Rydberg atoms, Nature Physics **16**, 857 (2020).

[64] H. C. J. Gan, G. Maslennikov, K.-W. Tseng, C. Nguyen, and D. Matsukevich, Hybrid Quantum Computing with Conditional Beam Splitter Gate in Trapped Ion System, Physical Review Letters **124**, 170502 (2020).

[65] H. Wang, Y.-H. Lai, Z. Yuan, M.-G. Suh, and K. Vahala, Petermann-factor sensitivity limit near an exceptional point in a Brillouin ring laser gyroscope, Nature Communications **11**, 1610 (2020).

[66] S. Khandelwal, N. Brunner, and G. Haack, Signatures of exceptional points in a quantum thermal machine, , 1 (2021), arXiv:2101.11553.